



ICCAE

**Military Technical College  
Kobry Elkobbah,  
Cairo, Egypt**

**7th International Conference  
On Civil & Architecture  
Engineering**

## **REHABILITATION OF MULTIPLE TUNNELS USING FILTER**

**M. N. Salem <sup>a\*</sup>, M. H. Mowafy <sup>b\*</sup>, H. M. El Deeb <sup>c\*</sup>**

<sup>a</sup> *Assoc. Prof., Water and Water Structures Eng. Dept.,*

<sup>b</sup> *Prof. of Water Structures, Head of Water and Water Structures Eng. Dept.,*

<sup>c</sup> *Assistant Lecturer, Water and Water Structures Eng. Dept.,*

<sup>\*</sup> *Faculty of Eng., Zagazig University, Zagazig, Egypt.*

Contact: Dr. Mohamed Nageeb Salem, Phone: 0552570104 - 0552575888  
Mobile: 0107333029E-mail: [mnsa30@yahoo.com](mailto:mnsa30@yahoo.com)

### **ABSTRACT**

Rehabilitation of old tunnels can be achieved through reduction of seepage forces on them using filters. In this case, the potential head on the outer surface of the tunnel can be reduced to reach zero. Circular tunnel rounded by filter known as (drainage-type tunnel) that permits flow through the filter around the tunnel. The special purpose computer program (Z-soil) is used to study seepage flow around single, double and triple tunnels rehabilitated by filters in homogeneous isotropic and anisotropic soils with different anisotropy ratio. The study includes the effect of the relative groundwater level, relative depth of the impermeable layer, relative depth of the tunnel under ground surface, and soil anisotropy ratio on the average seepage pressure around the tunnels. All the relations are presented in the form of dimensionless curves. The reduction in seepage pressure around single, double and triple tunnels resulting from the existence of filter are obtained.

### **KEYWORDS**

Seepage forces; Tunnel; Finite Element Method; Drainage-Type tunnel.

## 1. INTRODUCTION

The reduction of seepage pressure around existing tunnels is of great importance due to the wide engineering applications that can help in extending the working life of such tunnels. The present study deals with seepage flow around drainage-type tunnels coated by filters. Existence of filters around tunnels is intended to reduce the seepage forces around tunnels. It may be used in rehabilitation stage as maintenance for existing tunnels. Lee and Num (2001) studied the seepage force problems arising from the flow of groundwater into tunnels. Lee et al. (2003) studied the effect of seepage forces on the tunnel face stability. Callari (2004) presented an analysis of shallow tunneling in saturated poro-elastoplastic media. Lee et al. (2004) studied the effect of seepage forces on the tunnel face stability reinforced with multi-step pipe grouting. Lee and Num (2004) studied the effect of seepage forces arising from the groundwater flow on the tunnel face stability for underwater tunnels. Lee et al. (2006) studied the influence of seepage forces on the ground reaction curve of circular opening. Nam and Bobet (2006) studied the linear stresses in deep tunnels below the ground water table. Salem et al. (2007) studied the seepage forces around circular single drainage-type tunnel in homogenous and anisotropic soil with different anisotropy ratio.

Figure (1) shows a schematic representation of the studied tunnels including single, double, and triple tunnels along with their dimensions before rehabilitation. In the case of water-proof tunnel(s) there is now flow around tunnel(s) and the hydrostatic pressure at the tunnel center represented by  $p_c$ .

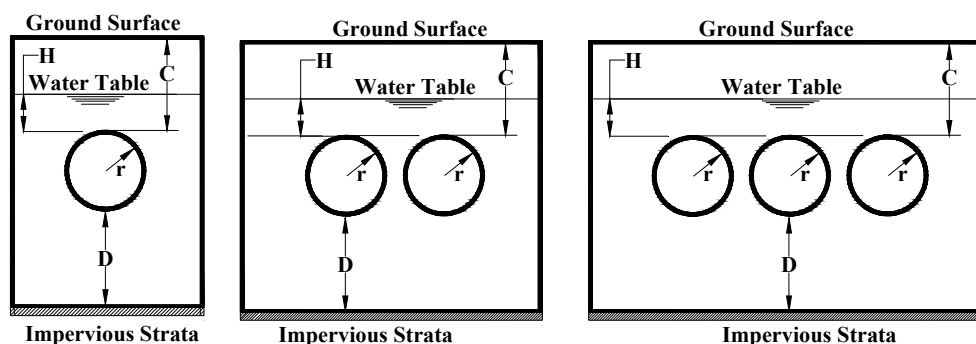


Figure (1): Single, double, and triple tunnels without filter, (before rehabilitation), including the domain dimensions.

In the case of existence of filter around the tunnel (rehabilitation stage), water moves through the filter around the tunnel towards the lower bottom, as shown in Figure (2). This flow movement reduces the piezometric head around the outer surface of the tunnel to zero.

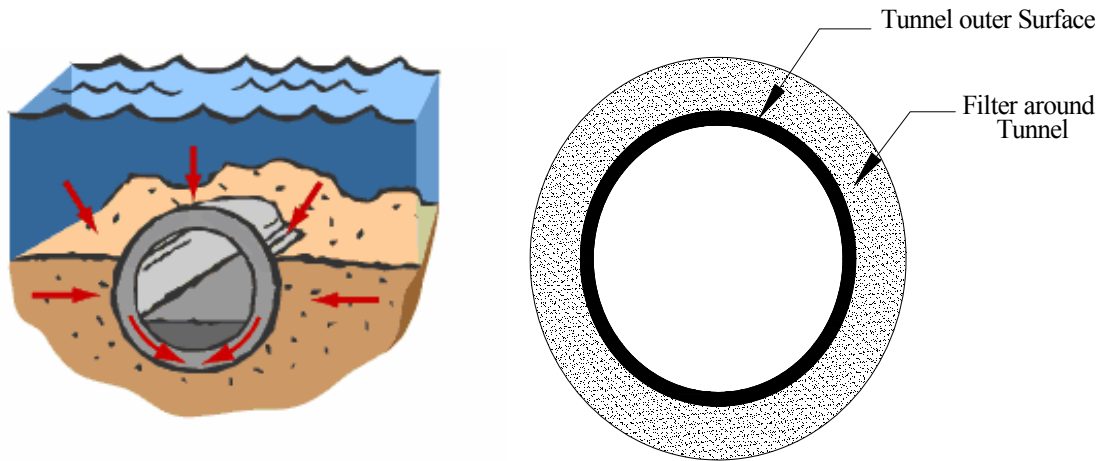


Figure (2): A single tunnel rounded by filter.

Figure (3) shows schematic representation of the studied tunnels after the rehabilitation stage with filters installed around the tunnels.

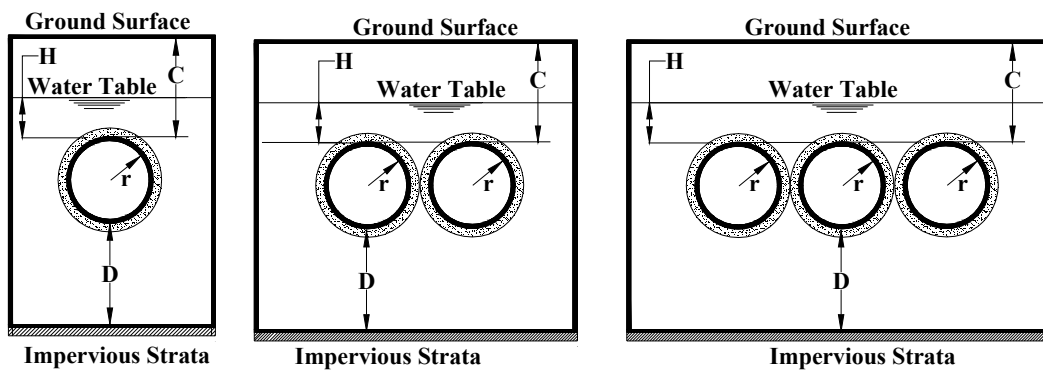


Figure (3): Single, double, and triple tunnel(s) rounded by filter, (after rehabilitation), including the domain dimensions.

## 2. BOUNDARY CONDITIONS

In studying the seepage flow around tunnels before and after the rehabilitation process, the following boundary conditions are applied, as shown in Figure (4):

*Type (i): Prescribed boundary,*

1- At the water table (groundwater) surface,  $h = h_0$ .

2- At the tunnel surface,  $h = 0$  in the case of existence of filter around the tunnel

*Type (ii): No flow across the impermeable surface,  $\frac{\partial h}{\partial n} = 0$ ,*

Where  $\mathbf{n}$  is the direction normal to the surface.

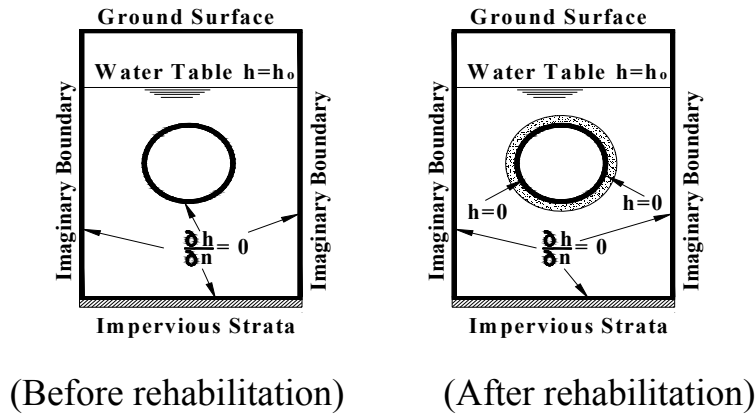


Figure (4): Boundary conditions before and after rehabilitation.

### 3. SEEPAGE FORCES

When the groundwater flows under steady-state flow conditions, there exists a difference in the hydraulic head from the surrounding ground to the tunnel lining. The force that acts on the soil grain due to the differential head is known as the *seepage force*, and it is exerted in the direction of groundwater flow.

The seepage force acting on a unit volume of soil grains can be expressed as,  $\mathbf{i} \cdot \gamma_w$ , where  $\gamma_w$  is the unit weight of water and,  $\mathbf{i}$ , is the hydraulic gradient. Consequently, to calculate the seepage force, the distribution of hydraulic head around the tunnel is first calculated by solving the groundwater flow equation using a two-dimensional Finite Element Program Z-Soil (2003). Next the hydraulic gradient was evaluated in each section followed by the seepage force.

By summing up all of the seepage forces, the total seepage force acting on the tunnel outer surface could be obtained. Then the average seepage pressure ( $p_{av}$ ) could be calculated by dividing the total seepage force by the tunnel surface area. Finally, the seepage pressure ratio ( $p_{av}/p_c$ ), which is the ratio of the average seepage pressure to the hydrostatic pressure at tunnel center is also calculated.

### 4. ANALYSIS OF THE RESULTS

Starting with the analysis of a single tunnel, Figures (5) and (6) represent the velocity distribution as velocity vectors and color shadow map, respectively through the domain of single tunnel rounded by filter. One half of the tunnel is analyzed due to symmetry. It is noticed that the flow moves towards the very bottom end of the tunnel and the maximum velocity reached **7.832 m/day**, occurring at that point, in the case of existence of filter around the tunnel.

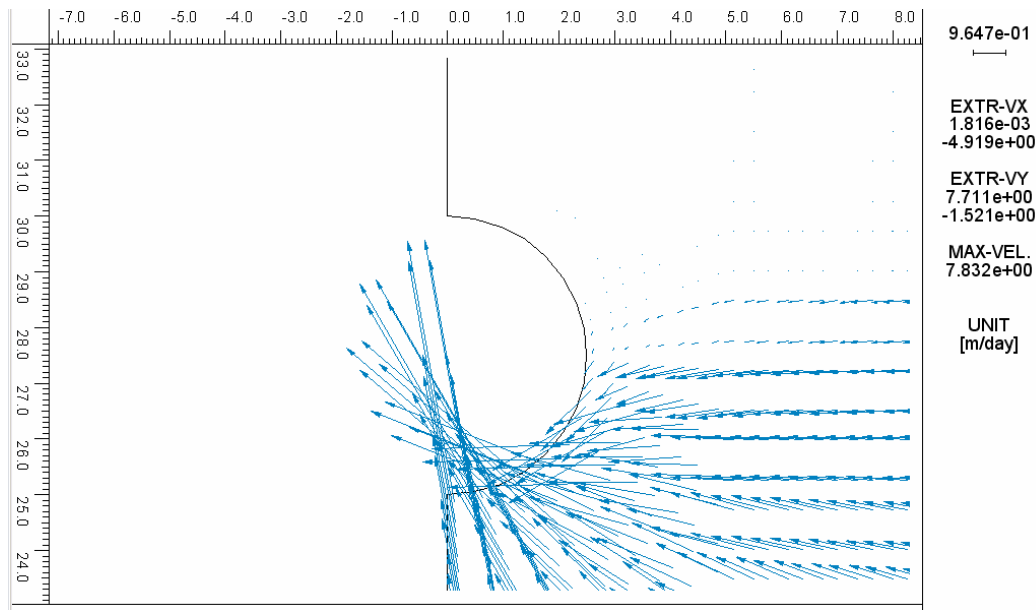


Figure (5): Velocity vectors distribution for a single tunnel (Z-soil Output), for ( $D/r = 10$ ,  $C/r = 3$  in homogeneous soil).

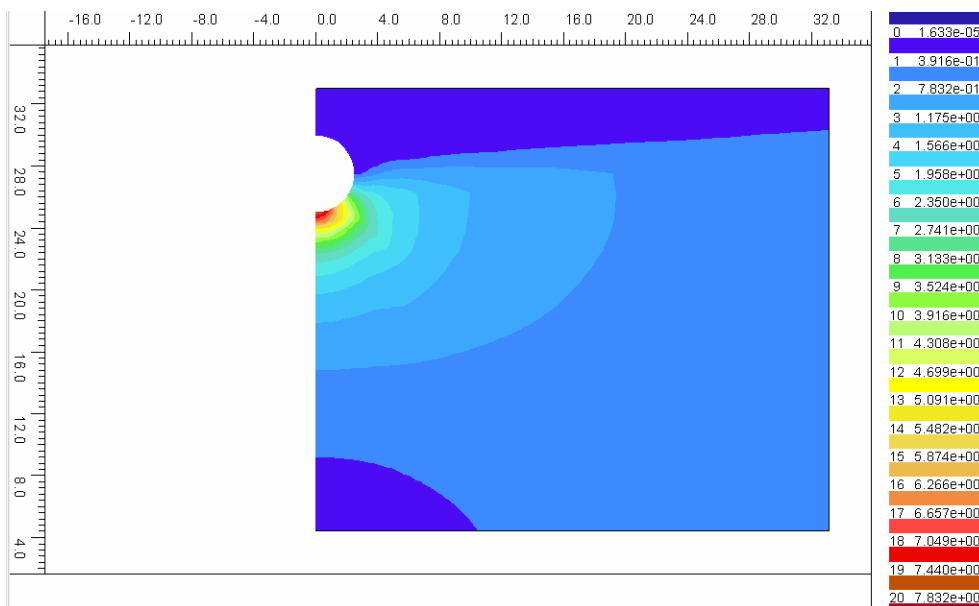


Figure (6): Velocity distribution for single tunnel as a color shadow map (Z-soil Output) for ( $D/r = 10$ ,  $C/r = 3$  in homogeneous soil).

Figures (7) and (8) represent the velocity distribution as vector and color shadow distributions, through the domain of double tunnels rounded by filters. The maximum velocity reduced to **6.849 m/day** occurs at the bottom end for each tunnel.

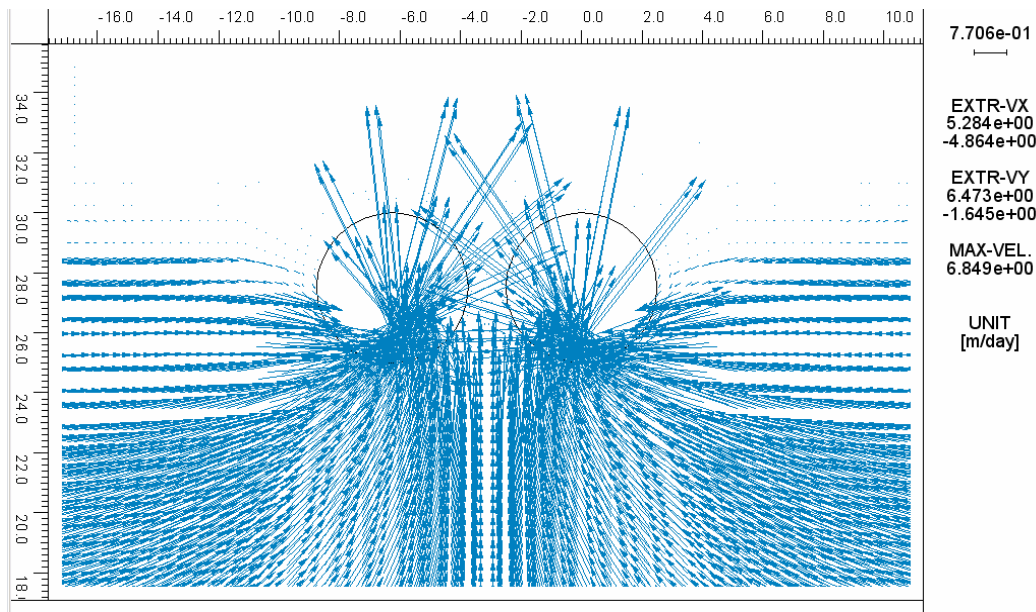


Figure (7): Velocity distribution for double tunnel (Z-soil Output) for ( $D/r = 10$ ,  $C/r = 3$  and homogeneous soil).

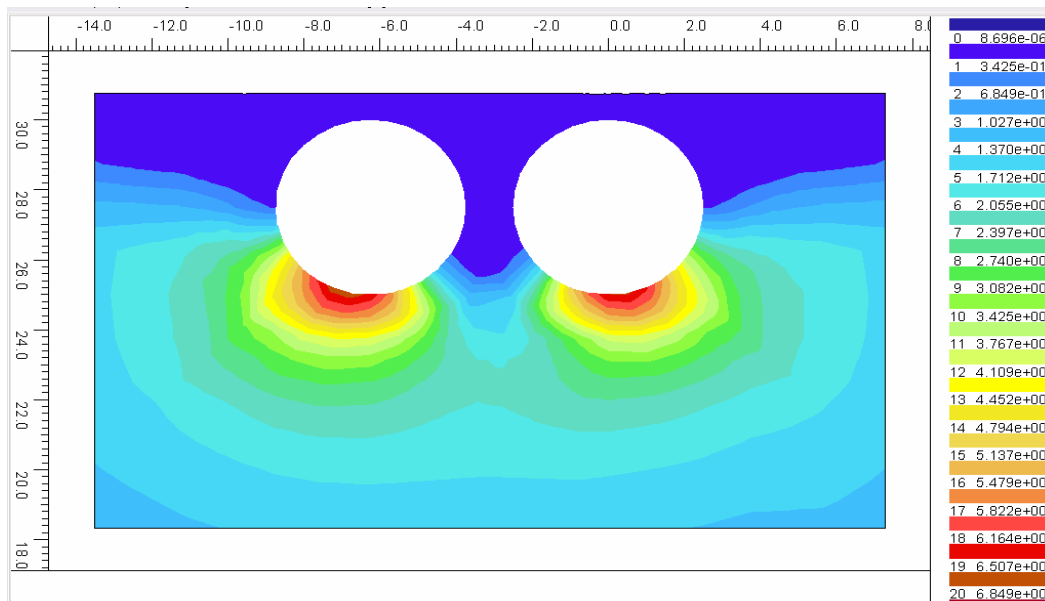


Figure (8): Velocity color shadow distribution for double tunnels (Z-soil Output), for ( $D/r = 10$ ,  $C/r = 3$  in homogeneous soil).

The case of three adjacent tunnels is shown in Figures (9) and (10) representing the velocity distribution around them. It is noticed that the maximum velocity further reduced to be 5.535 m/day.

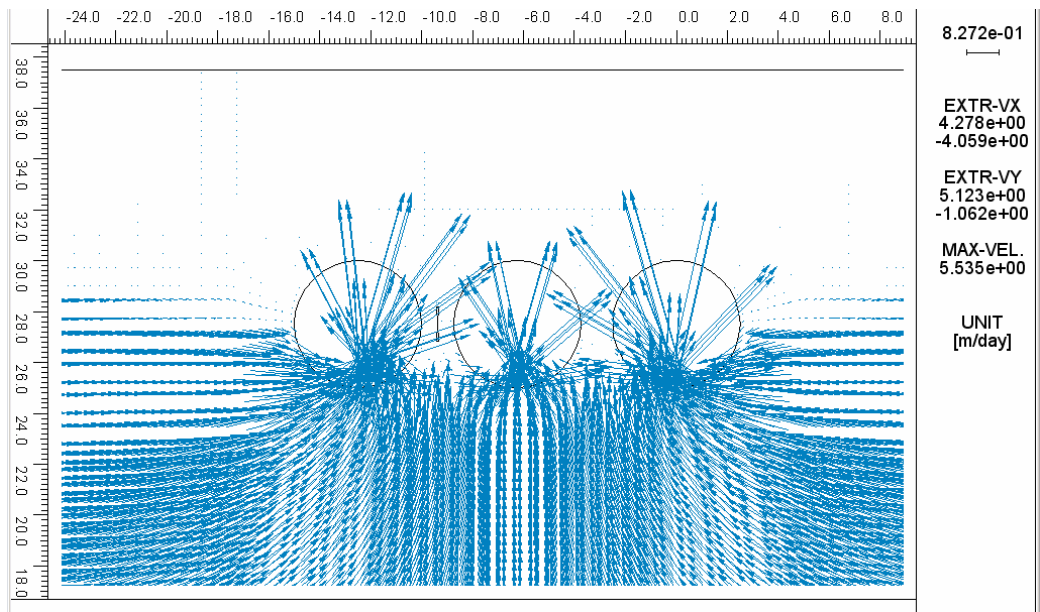


Figure (9): Velocity distribution for triple tunnels (Z-soil Output).  
( $D/r = 10$ ,  $C/r = 3$  and homogeneous soil).

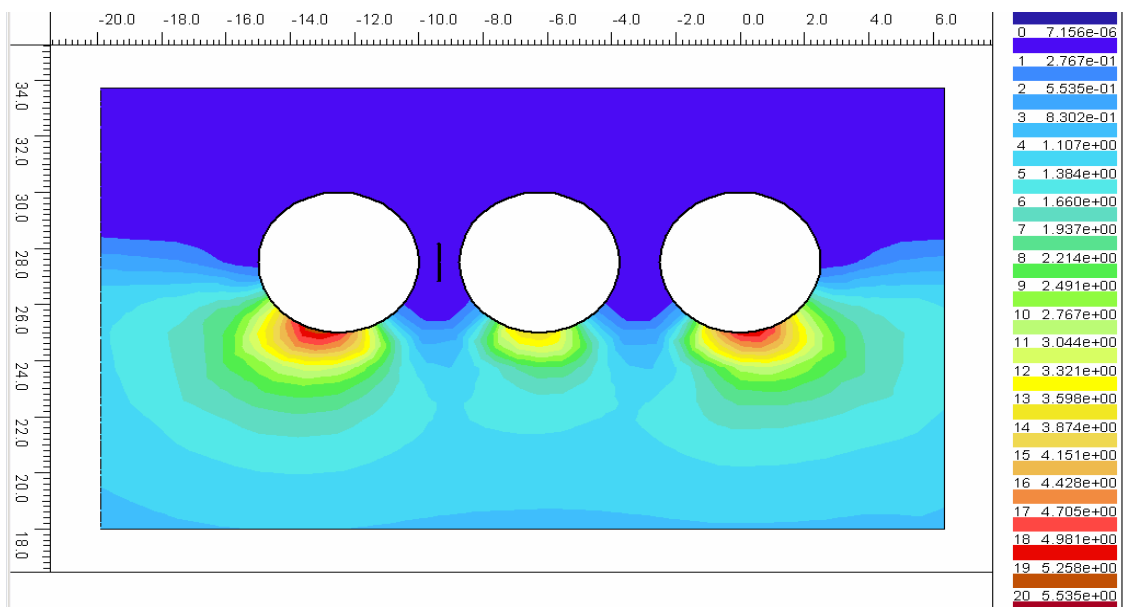


Figure (10): Velocity distribution for triple tunnel (Z-soil Output), as a color shadow map, for ( $D/r = 10$ ,  $C/r = 3$  and homogeneous soil).

Figure (11) represents the pressure ratio for single tunnel against the ground water level ratio,  $H/r$ , for different anisotropy ratio,  $K_x/K_y$  and impermeable layer depth,  $D/r = 10$ . About 15% decrease in seepage pressure as a result of decrease in ground water level ratio from 0.5 to 1.5 and still constant

after that. As  $K_x/K_y$  increases from 1 to 5, the seepage pressure ratio decreases. As  $K_x/K_y$  increases from 1 to 2 to 3 to 4 and to 5, the seepage pressure ratio decreases to be 20%, 11%, 7%, 5% respectively.

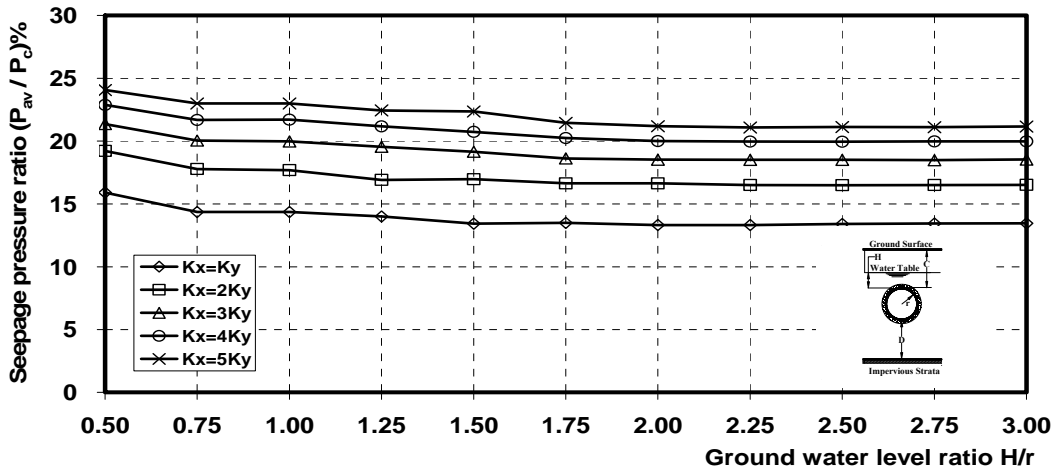


Figure (11): Seepage pressure ratio for different relative water tables with variation of anisotropy ratio ( $K_x/K_y$ ), and ( $D/r = 10$ ).

Figures (12) and (13) represent the previous relationships for impermeable layer depths,  $D/r = 15$  and  $D/r = 20$  respectively. It is noticed that as  $D/r$  increases to 15 as in Figure (12), the constant seepage pressure ratio starts at  $H/r = 1.75$ . As  $D/r$  increases to 20 the constant seepage pressure ratio starts at 2.0. The change in seepage pressure ratio for different  $K_x/K_y$  nearly the same as  $D/r = 10$ , as shown in Figure (13).

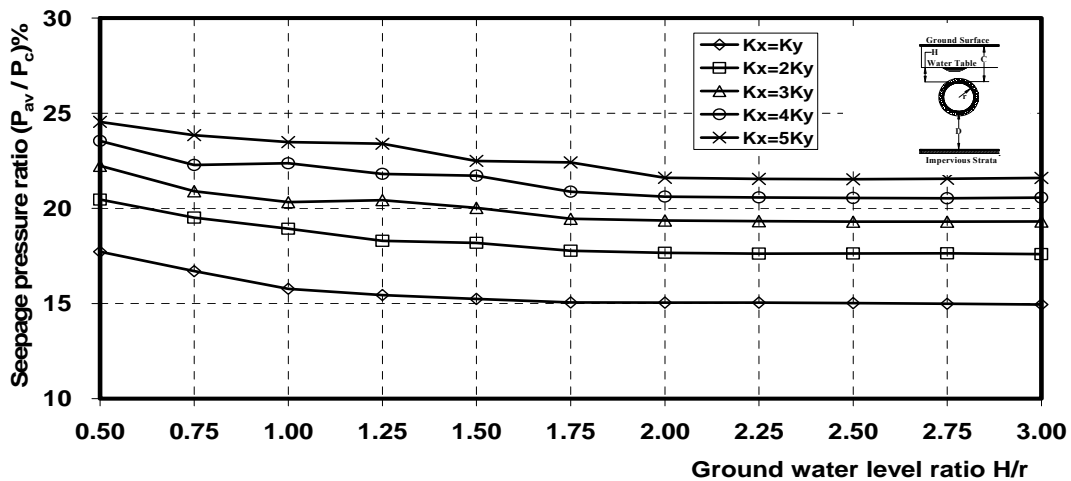


Figure (12): Seepage pressure ratio for different relative water tables with variation of anisotropy ratio ( $K_x/K_y$ ), and ( $D/r = 15$ ).



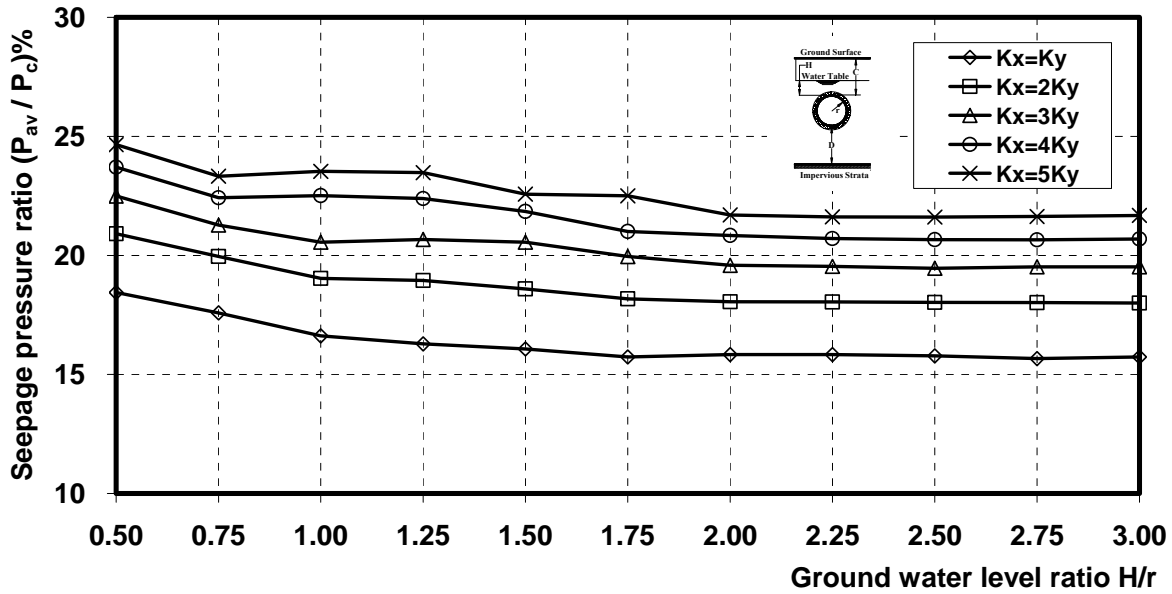


Figure (13): Seepage pressure ratio for different relative water tables with variation of anisotropy ratios ( $K_x/K_y$ ), and ( $D/r = 20$ ).

Figure (14) illustrates the seepage pressure ratio,  $p_{av}/p_c\%$ , versus the relative groundwater level ratio,  $H/r$ , for various anisotropy ratios,  $K_x/K_y$ . In this case, the relative depth of the tunnel ratio  $C/r$  equals 3. It is noticed that as  $H/r$  increases from 0.5 to 1.75 about 15% decrease in seepage pressure ratio is obtained. Constant seepage pressure is found thereafter. As the anisotropy ratio,  $K_x/K_y$ , increases from 1 to 5 the seepage pressure ratio increases. The rate of increase in the seepage pressure ratio,  $p_{av}/p_c$ , decreased as  $K_x/K_y$  increased.

Figure (15) and (16) represents the previous relationship for  $C/r = 4$  and  $C/r = 5$ , respectively.

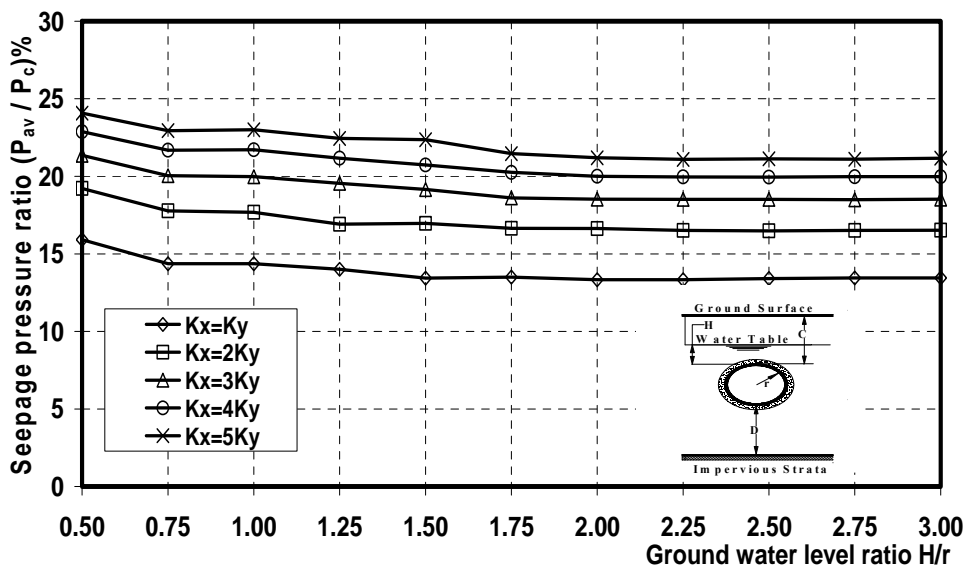


Fig.(14) Seepage pressure ratio for different relative water tables with variation of anisotropy ratio ( $K_x/K_y$ ), and ( $C/r = 3$ ).

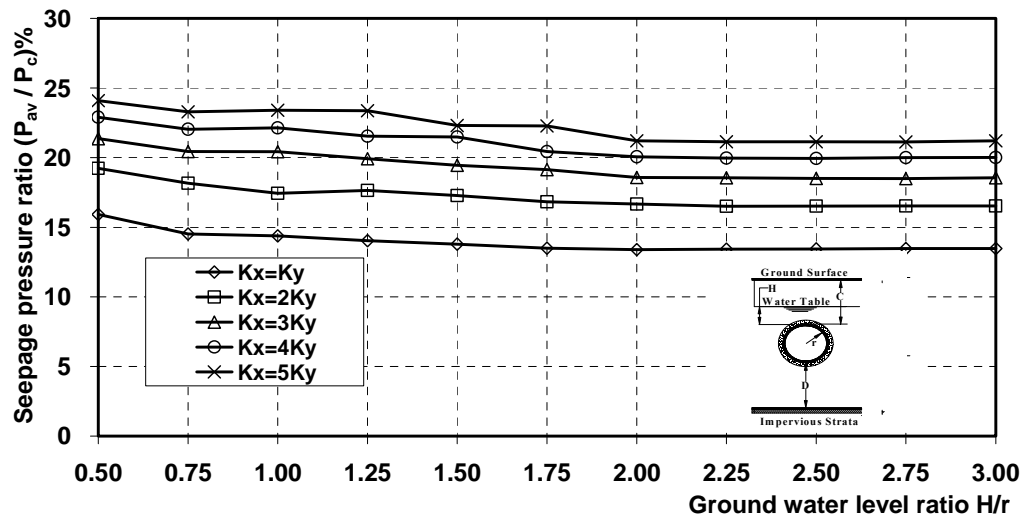


Figure (15): Seepage pressure ratio for different relative water tables with variation of anisotropy ratio ( $K_x/K_y$ ), and ( $C/r = 4$ ).

Figure (17) shows the seepage pressure ratio for different relative ground water heights,  $D/r = 10, 15$  and  $20$  in the case of two adjacent tunnels in homogeneous isotropic soil. It is noticed that as  $D/r$  increases from 10 to 15, about 15% decrease in the seepage pressure ratio took place. A reduction of 6% only in the seepage pressure ratio resulted from increasing  $D/r$  from 15 to 20. In addition, for each  $D/r$  ratio 21% reduction in seepage pressure is found as a result of increasing  $H/r$  from 0.5 to 3.0.

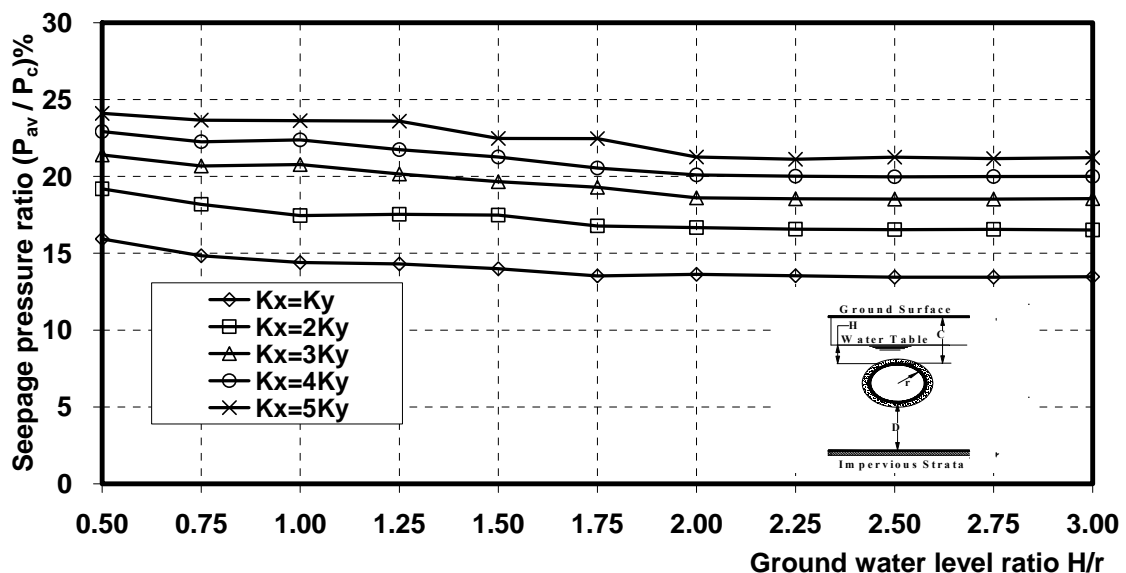


Figure (16): Seepage pressure ratio for different relative water tables with variation of anisotropy ratio ( $K_x/K_y$ ), and ( $C/r = 5$ ).

The seepage pressure ratio for different groundwater levels in the case of three adjacent tunnels is shown in Figure (18) that represents the middle tunnel only. It is noticed that about 29% and 9% increase in the seepage pressure ratios resulted from increasing D/r ratio from 10 to 15 and from 15 to 20, respectively at the groundwater level ratio, H/r, equal 0.5. As H/r increases from 0.5 to 3.0, the increase in seepage pressure ratio decreases to be 17% for H/r = 3. When increasing D/r from 15 to 20, the same increase, 9%, is obtained.

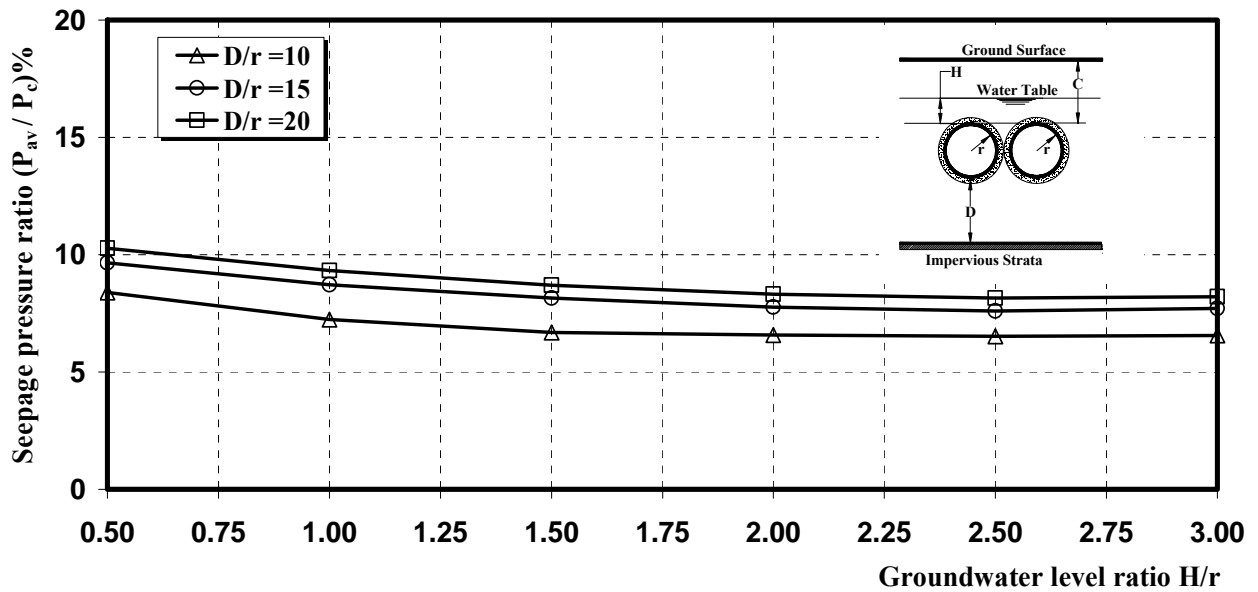


Figure (17): Seepage pressure ratio for different relative water tables, isotropic soil in case of two tunnels ( $K_x = K_y$ ).

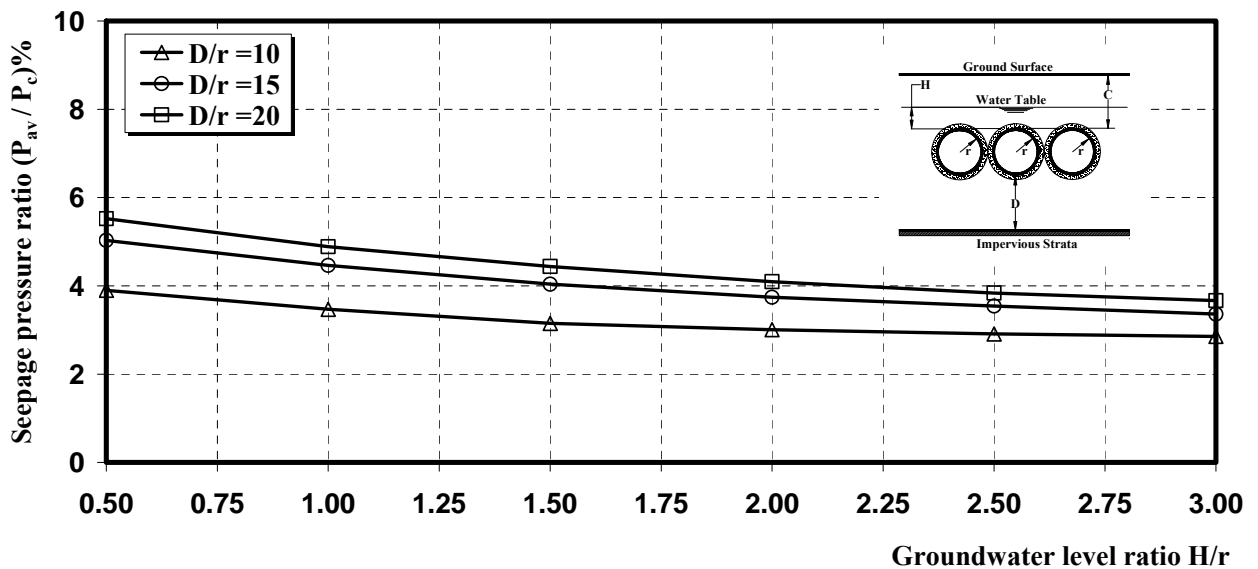


Figure (18): Seepage pressure ratio for different relative water tables for three adjacent tunnels (middle tunnel).

The seepage pressure ratio for different relative groundwater height, in the case of three adjacent tunnels, is represented in Figure (19) for the case of side tunnel. About 23% and 7% increase in the seepage pressure ratio is found as a result of increase in D/r from 10 to 15 and from 15 to 20, respectively.

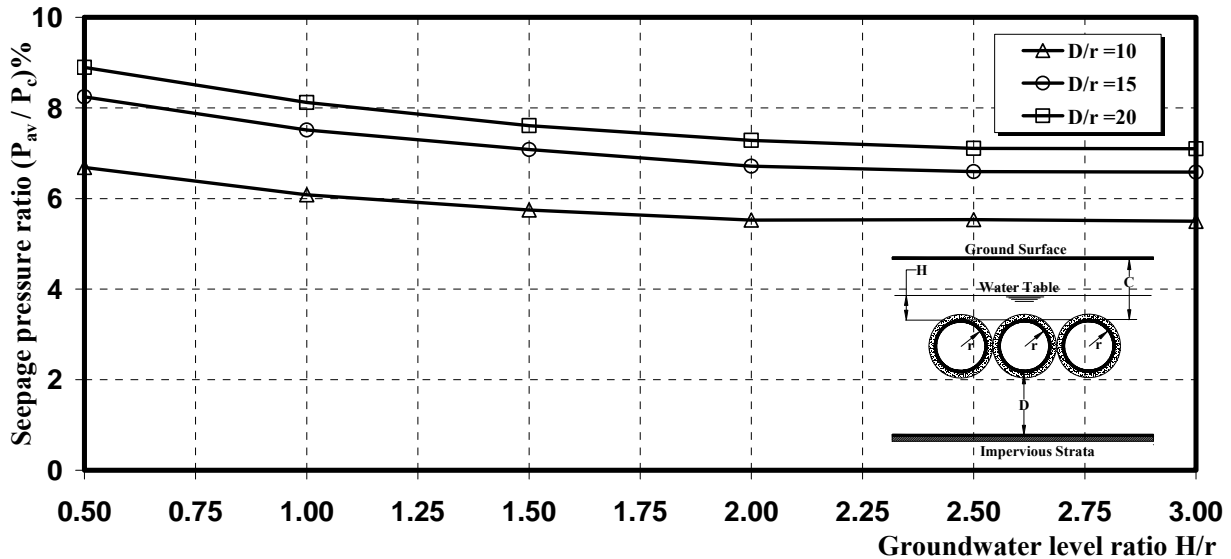


Figure (19): Seepage pressure ratio for different relative water tables for three adjacent tunnels (side tunnel).

Figure (20) illustrates the seepage pressure ratio for different relative groundwater height in the cases of single, two and three tunnels. The results is obtained for D/r = 10. In the case of double tunnels, the seepage pressure ratio decreased by 47% than that of single tunnel. More reduction occurs when three tunnels used, about 20% reduction in seepage pressure ratio in the case of side tunnel. About 53% reduction in the seepage pressure ratio in the middle tunnel of the values in the case of two tunnels. Figures (21) and (22) give the nearly similar results for D/r = 15 and 20 respectively.

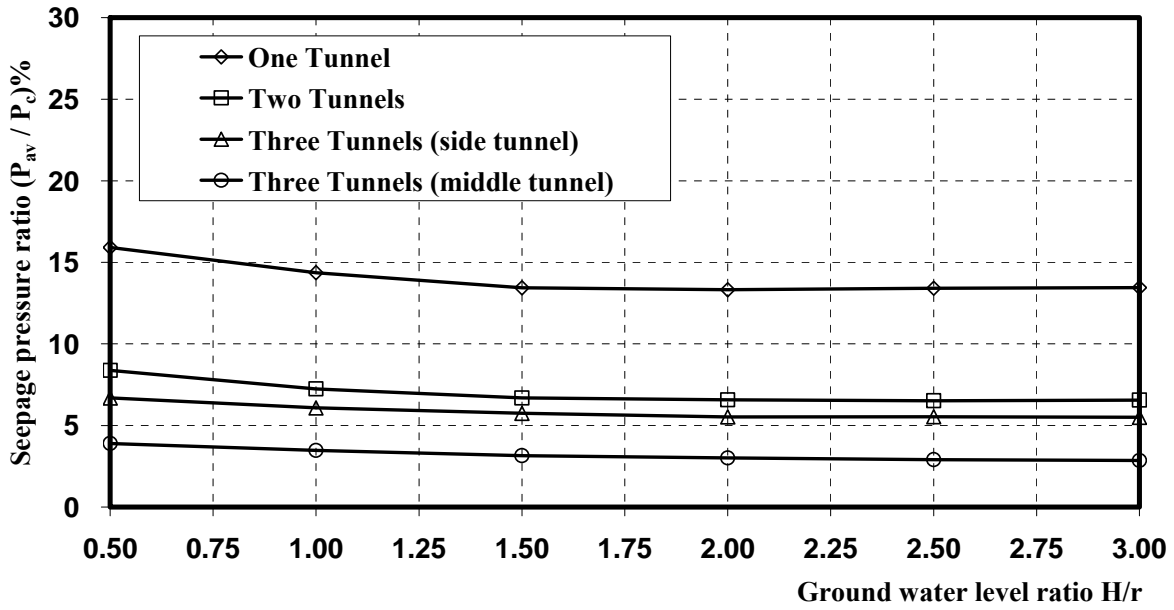


Figure (20): Seepage pressure ratio for different relative water tables, ( $D/r = 10$ ).

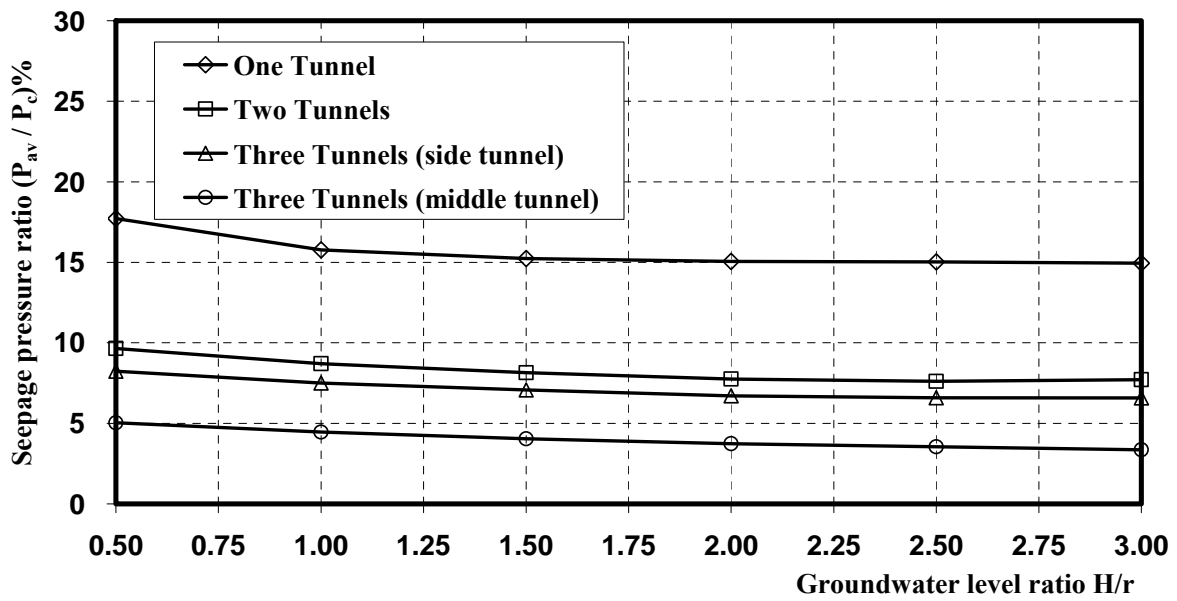


Figure (21): Seepage pressure ratio for different relative water tables, ( $D/r = 15$ ).

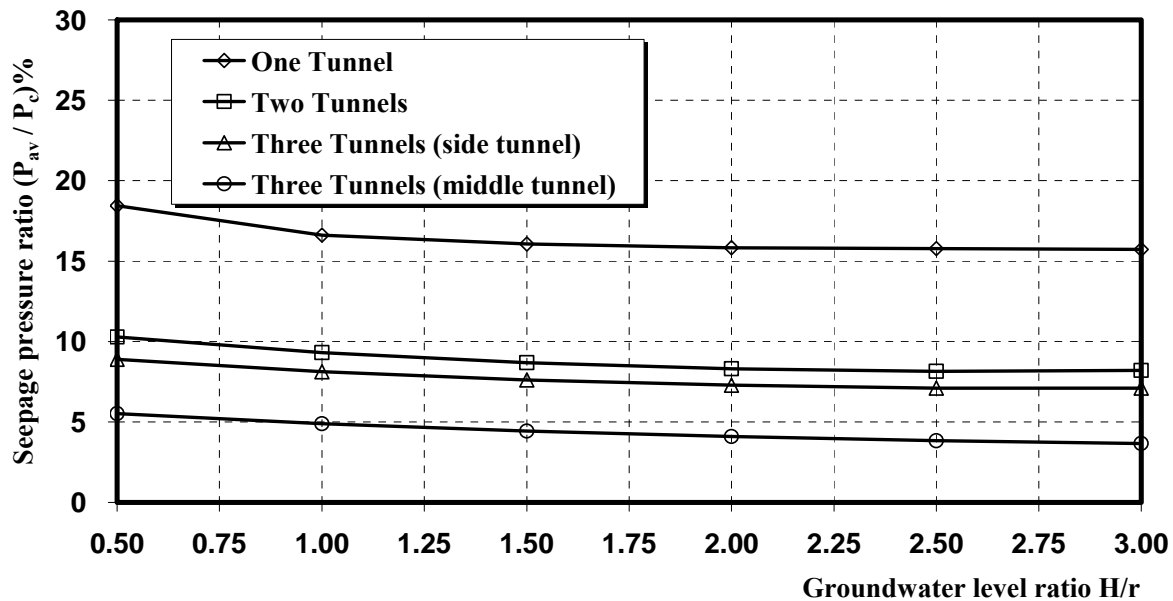


Figure (22): Seepage pressure ratio for different relative water tables, ( $D/r = 20$ ).

## 5. CONCLUSIONS

The following conclusions are drawn from the research results:

1. In the case of rehabilitation of water-proof tunnels by adding filter around them, the tunnels are changed to drainage-type tunnels. It could be unconservative to neglect the seepage forces resulting from flow through the filter rounding the tunnel lining into consideration.
2. The seepage pressure acting on the tunnel is proportional to the groundwater level. The ratio of the average seepage pressure to the hydrostatic pressure at tunnel center for the same groundwater level, named the seepage pressure ratio ( $p_{av}/p_c$ ), was about 15% for homogeneous isotropic soil and its average value was about 20% for homogeneous anisotropic soil for *one* tunnel. This means that the pressure reduced to be 15% and 20% of its original value for isotropic and anisotropic homogeneous soils as a result of placing of filter around the old single tunnel.
3. The pressure reduced to be about 8% of its original value for *two* adjacent circular drainage-type tunnels in homogeneous isotropic soil.
4. About 7% reduction in the original pressure for the *side* tunnels in the case of *three* adjacent circular drainage-type tunnels in homogeneous isotropic soil, but the reduction reaches 3.9% for the *middle* tunnel.
5. Increasing the adjacent tunnels number from *one* to *two* tunnels causes an average decrease in the seepage pressure ratio,  $p_{av}/p_c$ , by 47%.
6. Increasing the adjacent number of tunnels from *two* to *three* causes an average decrease in the seepage pressure ratio,  $p_{av}/p_c$ , by 53% for the *side* tunnels and 20% for the *middle* one.

7. Increasing the relative impermeable layer depth ratio ( $D/r$ ) causes an increase in seepage pressure ratio ( $p_{av}/p_c$ ). The rate of increment decreases as the relative impermeable layer depth ratio ( $D/r$ ) increases.
8. The increase of the relative ground surface height ratio ( $C/r$ ) has a small effect on seepage pressure ratio ( $p_{av}/p_c$ ) when the relative groundwater level ratio ( $H/r$ )  $< 2.0$ . However, when ( $H/r$ ) ratio  $\geq 2.0$ , the average seepage pressure ratios are constant for different relative ground surface height ratio ( $C/r$ ).
9. The increase in anisotropy ratio ( $K_x/K_y$ ) causes an increase in the average seepage ratio ( $p_{av}/p_c$ ). The rate of increment decreases as the anisotropy ratio ( $K_x/K_y$ ) increases.
10. The designer engineer may use of The seepage pressure ratio ( $p_{av}/p_c$ ) sdimensionless curves. These curves can be a simple estimation for the seepage pressure acting on the tunnel in homogeneous isotropic and anisotropic soils with different anisotropy ratio  $K_x/K_y = 2, 3, 4$  and  $5$ .

## 6. List of Symbols

Symbol	Definition
A	Cross-sectional area of soil mass, perpendicular to the direction of flow,
C	The ground surface height measured from tunnel crown,
C/r	The relative ground surface height ratio,
D	The impermeable layer depth measured from tunnel invert,
D/r	The relative impermeable layer depth ratio,
H	The groundwater level measured from tunnel crown,
H/r	The relative groundwater height ratio,
h	The field variable (hydraulic head),
h <sub>o</sub>	The hydrostatic head,
i	Hydraulic gradient,
K	Darcy's coefficient of permeability,
K <sub>x</sub>	Coefficient of permeability in x-direction,
K <sub>y</sub>	Coefficient of permeability in y-direction,
K <sub>x</sub> /K <sub>y</sub>	Anisotropy ratio,
P <sub>av</sub>	The average seepage pressure,
P <sub>c</sub>	The hydrostatic pressure at tunnel center,
P <sub>av</sub> /P <sub>c</sub>	The seepage pressure ratio,
r	Tunnel radius,
V	Velocity of flow,

## 7. REFERENCES

- 1- **Abdel Salam, M.E., (1985)**, "Grouting of alluvial soil in Cairo underground metro", Proceedings of the International Symposium on Tunneling in Soft and Water-Bearing Grounds, pp. 135-142.
- 2- **Atwa, M., and Leca, E., (1994)**, "Analysis of ground water seepage towards tunnels", Proceedings of the International Congress on Tunneling and Ground Conditions, Cairo, Egypt, April, pp. 303-310.
- 3- **Bindra, S.P., and Bindra, K., (1982)**, "Elements of Bridges, Tunnel and Railway Engineering", Dhanpat Rai & Sons.
- 4- **Callari, C., (2004)**, "Coupled numerical analysis of strain localization induced by shallow tunnels in saturated soils", Journal of Computers and Geotechnics, Vol. 31, pp. 193-207.
- 5- **El-Nahhas, F.M., (1999)**, "Soft Ground Tunneling in Egypt: Geotechnical Challenges and Expectations", Tunneling and Underground Space Technology, Vol. 14, No. 3, pp. 245-256.
- 6- **El-Tani, M., (2003)**, "Circular tunnel in a semi-infinite aquifer", Tunneling and Underground Space Technology, Vol. 18, pp. 49-55.
- 7- **Istok, J., (1989)**, "Groundwater modeling by the finite element method", American Geophysical Union. Water Resources Monograph.
- 8- **Lee, S.W., Jung, J.W., Nam, S.W., and Lee, I.M., (2006)**, "The influence of seepage forces on ground reaction curve of circular opening", Tunneling and Underground Space Technology.
- 9- **Lee, I.M., Lee, J.S., and Nam, S.W., (2004)**, "Effect of seepage force on tunnel face stability reinforced with multi-step pipe grouting", Tunneling and Underground Space Technology, Vol. 19, February, pp. 551-565.
- 10- **Lee, I.M., and Nam, S.W., (2001)**, "The study of seepage forces acting on the tunnel lining and tunnel face in shallow tunnels", Tunneling and Underground Space Technology, Vol. 16, February, pp. 31-40.
- 11- **Lee, I.M., and Nam, S.W., (2004)**, "Effect of tunnel advance rate on seepage forces acting on the underwater tunnel face", Tunneling and Underground Space Technology, Vol. 19, February, pp. 273-281.
- 12- **Lee, I.M., and Nam, S.W., (2006)**, "Seepage force considerations in tunneling", International Symposium on Underground Excavation and Tunneling, February, Bangkok, Thailand.
- 13- **Lee, I.M., Nam, S.W., and Ahn, J.H., (2003)**, "Effect of seepage forces on tunnel face stability", Canadian Geotechnical Journal, Vol. 40, February, pp. 342-350.
- 14- **Nam, S.W., and Bobet, A., (2006)**, "Liner stresses in deep tunnels below the water table", Tunneling and Underground Space Technology, Vol. 21, pp. 626-635.
- 15- **Otsuka, T., and Kamel, I.A., (1994)**, "Rehabilitation of Ahmed Hamdi Tunnel under the Suez Canal", Proceedings of the International Congress on Tunneling and Ground Conditions, Cairo, Egypt, April, pp. 601-608.



- 16-**Salem, M.N., (1994)**, "Analysis of flow under floors of hydraulic structures", Ph. D. Thesis, Zagazig University, Zagazig, Egypt.
- 17-**Salem, M.N., Mowafy, M.H., and El Deeb, H.M. (2007)**, "Effect of Seepage on Tunnels", V International Symposium on Environmental Hydrology, American Society of Civil Engineers-Egypt Section, Sep. 3-5, 2007, Cairo, Egypt.
- 18-**Terzaghi, K., and Peck, R.B., (1967)**, "Soil mechanics in engineering practice", 3<sup>rd</sup> Edition, John Wiley & Sons, Inc, New York.
- 19- **Z-Soil, (2003), ZACE services Ltd.**